BNL-81421-2008-JA, FERMILAB-PUB-08-301-CD-E, KEK/2008-25, TRIUMF/TRI-PP-08-04, TUHEP-EX-08-03

New measurement of the $K^+ \to \pi^+\nu\bar{\nu}$ branching ratio

A.V. Artamonov,[1] B. Bassalleck,[2] B. Bhuyan,[3,*] E.W. Blackmore,[4] D.A. Bryman,[5] S. Chen,[6,4] I-H. Chiang,[3] I.-A. Christidi,[7,†] P.S. Cooper,[8] M.V. Diwan,[3] J.S. Frank,[3] T. Fujiwara,[9] J. Hu,[4] J. Ives,[5] D.E. Jaffe,[3] S. Kabe,[10] S.H. Kettell,[3] M.M. Khabibullin,[11] A.N. Khotjantsev,[11] P. Kitching,[12] M. Kobayashi,[10] T.K. Komatsubara,[10] A. Konaka,[4] A.P. Kozhevnikov,[1] Yu.G. Kudenko,[11] A. Kushnirenko,[8,‡] L.G. Landsberg,[1,§] B. Lewis,[2] K.K. Li,[3] L.S. Littenberg,[3] J.A. Macdonald,[4,§] J. Mildenberger,[4] O.V. Mineev,[11] M. Miyajima,[13] K. Mizouchi,[9] V.A. Mukhin,[1] N. Muramatsu,[14] T. Nakano,[14] M. Nomachi,[15] T. Nomura,[9] T. Numao,[4] V.F. Obraztsov,[1] K. Omata,[10] D.I. Patalakha,[1] S.V. Petrenko,[1] R. Poutissou,[4] E.J. Ramberg,[8] G. Redlinger,[3] T. Sato,[10] T. Sekiguchi,[10] T. Shinkawa,[16] R.C. Strand,[3] S. Sugimoto,[10] Y. Tamagawa,[13] R. Tschirhart,[8] T. Tsunemi,[10,¶] D.V. Vavilov,[1] B. Viren,[3] Zhe Wang,[6,3] N.V. Yershov,[11] Y. Yoshimura,[10] and T. Yoshioka[10]

(E949 Collaboration)

[1] *Institute for High Energy Physics, Protvino, Moscow Region, 142 280, Russia*
[2] *Department of Physics and Astronomy, University of New Mexico, Albuquerque, NM 87131*
[3] *Brookhaven National Laboratory, Upton, NY 11973*
[4] *TRIUMF, 4004 Wesbrook Mall, Vancouver, British Columbia, Canada V6T 2A3*
[5] *Department of Physics and Astronomy, University of British Columbia, Vancouver, British Columbia, Canada V6T 1Z1*
[6] *Department of Engineering Physics, Tsinghua University, Beijing 100084, China*
[7] *Department of Physics and Astronomy, Stony Brook University, Stony Brook, NY 11794*
[8] *Fermi National Accelerator Laboratory, Batavia, IL 60510*
[9] *Department of Physics, Kyoto University, Sakyo-ku, Kyoto 606-8502, Japan*
[10] *High Energy Accelerator Research Organization (KEK), Oho, Tsukuba, Ibaraki 305-0801, Japan*
[11] *Institute for Nuclear Research RAS, 60 October Revolution Prospect 7a, 117312 Moscow, Russia*
[12] *Centre for Subatomic Research, University of Alberta, Edmonton, Canada T6G 2N5*
[13] *Department of Applied Physics, Fukui University, 3-9-1 Bunkyo, Fukui, Fukui 910-8507, Japan*
[14] *Research Center for Nuclear Physics, Osaka University, 10-1 Mihogaoka, Ibaraki, Osaka 567-0047, Japan*
[15] *Laboratory of Nuclear Studies, Osaka University, 1-1 Machikaneyama, Toyonaka, Osaka 560-0043, Japan*
[16] *Department of Applied Physics, National Defense Academy, Yokosuka, Kanagawa 239-8686, Japan*

(Dated: October 17, 2008)

Three events for the decay $K^+ \to \pi^+\nu\bar{\nu}$ have been observed in the pion momentum region below the $K^+ \to \pi^+\pi^0$ peak, $140 < P_\pi < 199$ MeV/c, with an estimated background of $0.93 \pm 0.17(\text{stat.})^{+0.32}_{-0.24}(\text{syst.})$ events. Combining this observation with previously reported results yields a branching ratio of $\mathcal{B}(K^+ \to \pi^+\nu\bar{\nu}) = (1.73^{+1.15}_{-1.05}) \times 10^{-10}$ consistent with the standard model prediction.

PACS numbers: 13.20.-v, 12.15.Hh

The decay $K^+ \to \pi^+\nu\bar{\nu}$ is among a handful of hadronic processes for which the decay rate can be accurately predicted in the standard model (SM) owing to knowledge of the transition matrix element from similar processes and minimal long-distance effects [1, 2]. The small predicted branching ratio, $\mathcal{B}(K^+ \to \pi^+\nu\bar{\nu}) = (0.85 \pm 0.07) \times 10^{-10}$ [3], and the fact that this decay is a flavor-changing neutral current process makes it a sensitive probe of a wide range of new physics effects [1]. Previous studies of this decay by experiment E787 at Brookhaven National Laboratory and its upgraded extension E949 have measured $\mathcal{B}(K^+ \to \pi^+\nu\bar{\nu}) = (1.47^{+1.30}_{-0.89}) \times 10^{-10}$ based on the observation of three events in a sample of 7.7×10^{12} K^+ decays at rest with a total expected background of 0.44 ± 0.05 events in the pion momentum region $211 < P_\pi < 229$ MeV/c above the $K^+ \to \pi^+\pi^0$ ($K_{\pi 2}$) peak (pnn1) [4, 5]. E787 set a consistent limit of $< 22 \times 10^{-10}$ at 90% C.L. based on one candidate in a sample of 1.7×10^{12} stopped K^+ decays with an expected background of 1.22 ± 0.24 events in the momentum region $140 < P_\pi < 195$ MeV/c below the $K_{\pi 2}$ peak (pnn2) [6, 7].

In this Letter we report the results of a search for $K^+ \to \pi^+\nu\bar{\nu}$ below the $K_{\pi 2}$ peak (pnn2) using 1.7×10^{12} stopped K^+ decays obtained with E949 as well as the final results on $\mathcal{B}(K^+ \to \pi^+\nu\bar{\nu})$ from E949 data combined with E787 data.

Identification of $K^+ \to \pi^+\nu\bar{\nu}$ decays relies on detection of an incoming kaon, its decay at rest and an outgoing pion with no coincident detector activity. The E949 apparatus and analysis of the data in the pnn1 region have been described elsewhere [5]. In this letter, we emphasize the apparatus and analysis features most relevant for pnn2.

Incoming kaons were identified by a Čerenkov counter and two proportional wire chambers before being slowed by an 11.1 cm thick BeO degrader and an active degrader,

passing through a beam hodoscope and stopping in the scintillating fiber target. Typically 1.6×10^6 K^+/s entered the target during a 2.2 s spill with a K^+/π^+ ratio of 3. The active degrader had 39 copper disks (2.2 mm thick) interleaved with 40 layers of 2 mm plastic scintillator divided into 12 azimuthal segments. Scintillation light from each segment was transported via wavelength shifting fibers to a photomultiplier tube (PMT) that was read out by time-to-digital convertors (TDCs), analog-to-digital convertors (ADCs) and GaAs CCD waveform digitizers (CCDs) sampling at 500 MHz [8]. The active degrader was capable of providing measurements of the incoming beam particle and activity concident with K^+ decay in the target. The target consisted of 413 scintillating fibers (5 mm square and 3.1 m long) packed into a 12 cm diameter cylinder. Each 5 mm fiber was connected to a PMT and read out by TDCs, ADCs and CCDs in order to record activity in the target coincident with both the incoming kaon and the outgoing pion.

The momentum and trajectory of the outgoing π^+ were measured in a drift chamber [9]. The outgoing pion came to rest in a range stack of 19 layers of plastic scintillator with 24 segments in azimuth. PMTs on each end of the scintillator were read out by TDCs, ADCs and 500-MHz transient digitizers [10] and enabled measurement of the pion range (R_π) and kinetic energy (E_π) as well as the $\pi^+ \to \mu^+ \to e^+$ decay sequence.

The barrel veto calorimeters of 16.6 radiation lengths (r.l.) at normal incidence provided photon detection over 2/3 of 4π sr solid angle. Photon detection over the remaining 1/3 of 4π sr solid angle was provided by a variety of calorimeters in the region from 10° to 45° of the beam axis with a total thickness from 7 to 15 r.l. [5, 11–13]. More extensive use was made by this analysis than the pnn1 analysis of the photon detection capabilities of the active degrader (6.1 r.l.) and the target (7.3 r.l.) that occupied the region within 10° of the beam axis.

This pnn2 analysis was able to increase the signal acceptance by 40% and maintain the same background rate per stopped K^+ as the previous analysis [7] thanks to improved background rejection primarily due to the addition of the active degrader and augmentation of the barrel veto by 2.3 r.l. for E949. In addition, the improved knowledge of the background contributions allowed the signal region to be divided into nine sub-regions ("cells"), with relative signal-to-background levels differing by a factor of 4, that were used in the likelihood method [14] to determine $\mathcal{B}(K^+ \to \pi^+\nu\bar{\nu})$.

To avoid a possible bias, we employed a "blind analysis" technique [5] in which the signal region was not examined until all selection criteria ("cuts") for signal had been established, the estimates of all backgrounds completed and acceptance of all cells determined. Two uncorrelated cuts with significant rejection were developed for most backgrounds. After imposing basic event quality cuts, inversion of one of the pair of cuts could then be used to select a background-enriched data sample containing N events. Inversion of the complementary cut selected a data sample on which the rejection $\mathcal{R}$ of the first cut could be measured. The background was estimated as $N/(\mathcal{R}-1)$. We ensured unbiased background estimates by dividing the data into one-third and two-thirds samples chosen uniformly from the entire data set. Selection criteria were determined with the one-third sample and background levels were measured from the two-thirds sample. In contrast to the analysis of the pnn1 region, some backgrounds did not have sufficiently distinct characteristics to permit isolation by cut inversion of a pure background sample and permit a measurement of $\mathcal{R}$ with the data. For these backgrounds, $\mathcal{R}$ was estimated with simulated data as described below.

Process	Background events
$K_{\pi 2}$ target-scatter	$0.619 \pm 0.150^{+0.067}_{-0.100}$
$K_{\pi 2}$ range-stack-scatter	$0.030 \pm 0.005 \pm 0.004$
$K_{\pi 2\gamma}$	$0.076 \pm 0.007 \pm 0.006$
K_{e4}	$0.176 \pm 0.072^{+0.233}_{-0.124}$
Charge-exchange	$0.013 \pm 0.013^{+0.010}_{-0.003}$
Muon	0.011 ± 0.011
Beam	0.001 ± 0.001
Total	$0.927 \pm 0.168^{+0.320}_{-0.237}$

TABLE I: Summary of the estimated number of events in the signal region from each background component. Each component is described in the text.

Table I summarizes the estimated background levels. The largest background was due to $K_{\pi 2}$ decays in which the π^+ scatters in the target, losing energy and obscuring the directional correlation with the photons from the π^0 decay that would otherwise be detected in the barrel veto. Two cuts that suppressed this background were 1) identification of π^+ scattering and 2) detection of the photons from π^0 decay. Pion scattering was identified by kinks in the pattern of target fibers attributed to the pion, by tracks that did not point back to the fiber containing the K^+ decay, by energy deposits inconsistent with an outgoing pion or by unexpected energy deposits at the time of the pion in fibers traversed by the kaon. The target pulse-shape cut identified the latter signature by performing a least-squares fit to the CCD samples to identify the pulses due to activity coincident with the kaon or pion [7]. The uncertainty in the $K_{\pi 2}$ target-scatter background had comparable statistical and systematic contributions. The systematic uncertainty was determined by the range of photon veto rejection values measured on samples of $K_{\pi 2}$ scatter events selected by different scattering signatures in the target or in different π^+ kinematic regions [15]. There was also a much smaller background from $K_{\pi 2}$ due to scattering in the range stack that was similarly identified by the energy deposits and pattern of range stack counters attributed to the track.

Additional backgrounds included $K^+ \to \pi^+\pi^-e^+\nu$ (K_{e4}), $K^+ \to \pi^+\pi^0\gamma$ ($K_{\pi2\gamma}$), $K^+ \to \mu^+\nu$, $K^+ \to \mu^+\nu\gamma$ and $K^+ \to \pi^0\mu^+\nu$ (muon), scattered beam pions (beam) and π^+ resulting from K^+ charge-exchange reactions dominated by $K^0_{\rm L} \to \pi^+\mu^-\bar{\nu}$. Simulated data were used to estimate the rejection $\mathcal{R}$ of the cuts that suppress K_{e4}, $K_{\pi2\gamma}$ and charge-exchange backgrounds. The K_{e4} and $K_{\pi2\gamma}$ backgrounds could not be distinguished from the larger $K_{\pi2}$-scatter background based solely on the π^+ track, and it was not possible to isolate a sufficiently pure, statistically significant sample of charge-exchange events on which to measure $\mathcal{R}$.

The K_{e4} process forms a background when the π^- and e^+ interact in the target without leaving a detectable trace. Positron interactions were well-modelled in our EGS4-based simulation [16] and we used the π^- energy deposition spectrum in scintillator measured previously in E787 [17] to model π^- absorption. We assessed the systematic uncertainty in the K_{e4} background by varying the threshold of cuts on the energy deposited in the target fibers at the time of the pion. The kinematics cuts defining the signal region were $140 < P_\pi < 199$ MeV/c, $60 < E_\pi < 100.5$ MeV and $12 < R_\pi < 28$ cm. We defined a sub-region $165 < P_\pi < 197$ MeV/c, $72 < E_\pi < 100$ MeV and $17 < R_\pi < 28$ cm where the lower and upper limits were chosen to suppress the K_{e4} background that peaks near 160 MeV/c and the tail of the $K_{\pi2}$ peak, respectively.

The rejection of the $K_{\pi2\gamma}$ background was calculated using a combination of simulated $K_{\pi2}$ and $K_{\pi2\gamma}$ events and $K_{\pi2}$ data events. The additional photon veto rejection due to the radiative photon was calculated from the photon distribution in simulated events and the rejection power of single photons as a function of angle and energy evaluated with $K_{\pi2}$ data [18].

Measurements of $K^0_{\rm S} \to \pi^+\pi^-$ decay from the K^+ charge-exchange reaction were used as input to simulate charge-exchange events [5]. The requirement on the delayed coincidence between the reconstructed kaon and pion candidates provided suppression of charge-exchange background as the emitted π^+ was required to originate within the fiducial region of the target. The systematic uncertainty was assessed with the same methodology as the K_{e4} background.

The muon and beam backgrounds were estimated entirely from data and were very small. As previous analyses had shown the muon background to be small [6, 7], the transient-digitizer-based cuts on $\pi^+ \to \mu^+ \to e^+$ identification were loosened to gain about 10% in acceptance. The total acceptance of the signal region was $(1.37 \pm 0.14) \times 10^{-3}$.

In order to explore and verify the reliability of the background estimates, we examined three distinct data regions just outside the signal region by loosening the photon veto (PV_n) or target pulse-shape (CCD_n) cut. Each of the two regions, PV_1 and CCD_1, were immediately adjacent to the signal region while a third region PV_2, adjacent to PV_1, was defined by further loosening of the photon veto cut. The number of expected and observed events and the probability of the observation are given in Table II. The 5% probability for the regions nearest the signal region may have indicated that the background was over-estimated. Given the inability to cleanly isolate each background component by cut inversion, some contamination (i.e. events due to backgrounds from other sources) is possible and would generally inflate the background estimates. Re-evaluation of the probabilities at the lower limit of the systematic uncertainties [15] gave 14% for the two closest regions and demonstrated that the assigned systematic uncertainties were reasonable.

Region	$N_{\rm E}$	$N_{\rm O}$	$\mathcal{P}(N_{\rm O}; N_{\rm E})$	Combined
CCD_1	$0.79^{+0.46}_{-0.51}$	0	0.45 [0.29,0.62]	NA
PV_1	$9.09^{+1.53}_{-1.32}$	3	0.02 [0.01,0.05]	0.05 [0.02,0.14]
PV_2	$32.4^{+12.3}_{-8.1}$	34	0.61 [0.05,0.98]	0.14 [0.01,0.40]

TABLE II: Comparison of the expected ($N_{\rm E}$) and observed ($N_{\rm O}$) number of background events in three regions CCD_1, PV_1 and PV_2 outside the signal region. The central value of $N_{\rm E}$ is given along with the combined statistical and systematic uncertainties. $\mathcal{P}(N_{\rm O}; N_{\rm E})$ is the probability of observing $N_{\rm O}$ events or fewer when $N_{\rm E}$ events are expected. The rightmost column "Combined" gives the probability of the combined observation in that region and the region(s) of the preceding row(s). The numbers in square brackets are the probabilities re-evaluated at the upper and lower bounds of the uncertainty on $N_{\rm E}$ [15].

After completion of the background studies, the signal region was examined and three candidates were found. The energy *vs.* range for these observed candidates is shown in Figure 1 along with the results of previous E787 [6, 7] and E949 [4, 5] analyses. From these three new events alone, $\mathcal{B}(K^+ \to \pi^+\nu\bar{\nu}) = (7.89^{+9.26}_{-5.10}) \times 10^{-10}$ was calculated using the likelihood method [14] assuming the SM spectrum and taking into account the uncertainties in the background and acceptance measurements [19]. When combined with the results of previous E787 and E949 analyses, we found $\mathcal{B}(K^+ \to \pi^+\nu\bar{\nu}) = (1.73^{+1.15}_{-1.05}) \times 10^{-10}$. The signal-to-background (S/B) ratios for the three events are 0.20, 0.42 and 0.47 [20], which can be compared with the S/B = 0.20 for the previous pnn2 candidate [6] and with the S/B = 59, 8.2 and 1.1 for the pnn1 events [4] assuming $\mathcal{B}(K^+ \to \pi^+\nu\bar{\nu}) = 1.73 \times 10^{-10}$. In this analysis, a candidate in the best (worst) cell would have had S/B=0.84 (0.20). The probability that the three new events were due to background only, given the estimated background in each cell, is 0.037. The probability that all seven $K^+ \to \pi^+\nu\bar{\nu}$ events were due to background is 0.001. In summary, these observations imply a $K^+ \to \pi^+\nu\bar{\nu}$ branching ratio consistent with SM expectations.

We acknowledge the dedicated effort of the technical

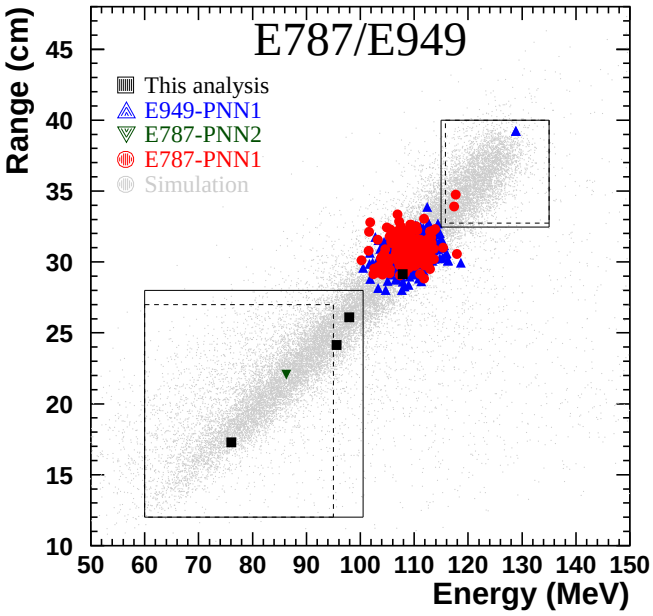

FIG. 1: Kinetic energy *vs.* range of all events passing all other cuts. The squares represent the events selected by this analysis. The circles and upward-pointing triangles represent the events selected by the E787 and E949 pnn1 analyses, respectively. The downward-pointing triangles represent the events selected by the E787 pnn2 analyses. The solid (dashed) lines represent the limits of the pnn1 and pnn2 signal regions for the E949 (E787) analyses. Despite the smaller signal region in E_π *vs.* R_π, the pnn1 analyses were 4.2 times more sensitive than the pnn2 analyses. The points near $E_\pi = 108$ MeV were $K_{\pi 2}$ decays that survived the photon veto cuts and were predominantly from the pnn1 analyses due to the higher sensitivity and the less stringent photon veto cuts. The light gray points are simulated $K^+ \to \pi^+ \nu\bar{\nu}$ events that would be accepted by our trigger.

staff supporting E949, the Brookhaven C-A Department, and the contributions made by colleagues who participated in E787. This research was supported in part by the U.S. Department of Energy, the Ministry of Education, Culture, Sports, Science and Technology of Japan through the Japan-U.S. Cooperative Research Program in High Energy Physics and under Grant-in-Aids for Scientific Research, the Natural Sciences and Engineering Research Council and the National Research Council of Canada, the program for New Century Excellent Talents in University from the Chinese Ministry of Education, the Russian Federation State Scientific Center Institute for High Energy Physics, and the Ministry of Industry, Science and New Technologies of the Russian Federation.

* Now at Department of Physics, Indian Institute of Technology Guwahati, Guwahati, Assam, 781 039, India.
† Now at Physics Department, Aristotle University of Thessaloniki, Thessaloniki 54124, Greece
‡ Now at Institute for High Energy Physics, Protvino, Moscow Region, 142 280, Russia.
§ Deceased.
¶ Now at Department of Physics, Kyoto University, Sakyo-ku, Kyoto 606-8502, Japan.

[1] A. J. Buras, F. Schwab, and S. Uhlig, Rev. Mod. Phys. **80**, 965 (2008), hep-ph/0405132.
[2] F. Mescia and C. Smith, Phys. Rev. **D76**, 034017 (2007), arXiv:0705.2025.
[3] J. Brod and M. Gorbahn, Phys. Rev. **D78**, 034006 (2008), arXiv:0805.4119. The uncertainty in the prediction is dominated by the uncertainty in the elements of the CKM matrix.
[4] V. V. Anisimovsky et al., Phys. Rev. Lett. **93**, 031801 (2004), hep-ex/0403036.
[5] S. Adler et al., Phys. Rev. **D77**, 052003 (2008), arXiv:0709.1000.
[6] S. Adler et al., Phys. Lett. **B537**, 211 (2002), hep-ex/0201037.
[7] S. Adler et al., Phys. Rev. **D70**, 037102 (2004), hep-ex/0403034.
[8] D. A. Bryman et al., Nucl. Instrum. Meth. **A396**, 394 (1997).
[9] E. W. Blackmore et al., Nucl. Instrum. Meth. **A404**, 295 (1998).
[10] M. Atiya, M. Ito, J. Haggerty, C. Ng, and F. W. Sippach, Nucl. Instrum. Meth. **A279**, 180 (1989).
[11] I. H. Chiang et al., IEEE Trans. Nucl. Sci. **42**, 394 (1995).
[12] T. K. Komatsubara et al., Nucl. Instrum. Meth. **A404**, 315 (1998).
[13] O. Mineev et al., Nucl. Instrum. Meth. **A494**, 362 (2002), physics/0207033.
[14] T. Junk, Nucl. Instrum. Meth. **A434**, 435 (1999), hep-ex/9902006.
[15] This method of assigning systematic uncertainty was intended to define a range that included the actual value of the background.
[16] W. R. Nelson, H. Hirayama, and D. W. O. Rogers (1985), SLAC-0265.
[17] M. Ardebili, Ph.D. thesis, Princeton University (1995), UMI-95-27860.
[18] K. Mizouchi, Ph.D. thesis, Kyoto University (2006).
[19] J. Ives, Ph.D. thesis, University of British Columbia, to be published.
[20] The kinetic energies of the events with S/B of 0.20, 0.42 and 0.47 were 76.1, 97.9 and 95.6 MeV, respectively.